ELSEVIER

Journal of Organometallic Chemistry 497 (1995) 91–104

Journal of Organometallic Chemistry

A density functional study on the insertion mechanism and chain termination in Kaminsky-type catalysts; comparison of frontside and backside attack ☆

John C.W. Lohrenz [a], Tom K. Woo [a], Liangyou Fan [b], Tom Ziegler [a,*]

[a] *Department of Chemistry, University of Calgary, 2500 University Drive N.W., Calgary, Alberta T2N 1N4, Canada*
[b] *Novacor Research and Technology Corporation, 2928-16 Street N.E., Calgary, Alberta T2E 7K7, Canada*

Received 2 January 1995

Abstract

Non-local density functional (DF) calculations have been carried out on the reaction of ethylene with Cp_2Zr^+–Et, which serves as a model for the resting state between two insertions. The β-agostic Cp_2Zr^+–Et is 47.0 kJ mol^{-1} more stable than the α-agostic conformer. Frontside insertion of the olefin can take place after rotation around the Zr–C_α-bond forming the α-agostic Cp_2Zr^+–Et. An α-agostic π-complex is formed with a complexation energy of 81.1 kJ mol^{-1} and the frontside transition state has an activation energy of 2 kJ mol^{-1} relative to the π-complex. The reaction is exothermic by 118.9 kJ mol^{-1}. Without rotation around the Zr–C_α bond a β-agostic π-complex is formed and H-transfer from the polymer chain end to the olefin takes place. This reaction leads to chain termination with an activation barrier of 29.8 kJ mol^{-1}. An alternative path for the olefin insertion starts with a backside attack of the olefin. The activation barrier for the backside insertion is 28.9 kJ mol^{-1} and the reaction is exothermic by 24.9 kJ mol^{-1} relative to the π-complex. Backside insertion does not involve inversion at the metal centre. The formation of syndiotactic polypropene in the case of the backside insertion can only be explained with chain-end control. Comparison of three chain termination processes (β-hydride elimination, C–H activation and H-exchange) indicates that H-exchange is the most probable reaction. β-Elimination is strongly endothermic and frontside C–H-activation makes a rotation around Zr–C_α necessary.

Keywords: Density functional study; Kaminsky-type catalysts; Mechanistic study; Early transition metals

1. Introduction

Over the last ten years the interest in homogeneous metallocene [1–9] based catalysts for olefin polymerization has grown and it is expected that over the next several years these catalysts will partially replace conventional Ziegler–Natta catalyst systems. Metallocene catalysts have several desirable properties, such as high activity, high stereoselectivity, and an ability to produce high-molecular-weight polymers with a narrow molecular-weight distribution. Furthermore, it is possible to fine tune properties such as the stereoselectivity by tailoring the metallocene ligands. For example, it is possible to polymerize propene to form *iso*-, *syndio*-, and *hemiisotactic* polypropene.

The catalysts are usually generated from dichloro metallocenes through a reaction with excess methylaluminoxane (MAO) as introduced by Kaminsky and Sinn in 1976 [1]. Stereoregular polymers by homogeneous catalysis were first obtained by Kaminsky and Brintzinger in 1984 [2], who used stereorigid C_2-symmetric *ansa*-metallocenes such as **1** for the synthesis of *isotactic* polypropene. In 1988 Ewen [3] was able to produce *syndiotactic* polypropene with a system based on the C_s-symmetric catalyst **2**.

Most systems are based on zirconium but titanocenes as well as hafnocenes [3] have been investigated. Further metals applied are scandium [10,11], lanthanides [12,13], chromium [14,15] and some Group VIII metals [16,17].

Jordan [18–21] investigated the nature of the active catalyst and was able to show that in case of the Group IV metallocenes the active species is a cationic alkyl complex with a vacant coordination site. From this it

☆ Dedicated to Professor Dr. Hans-Herbert Brintzinger on the occasion of his 60th birthday.

* Corresponding author.

SSDI 0022-328X(95)00110-7

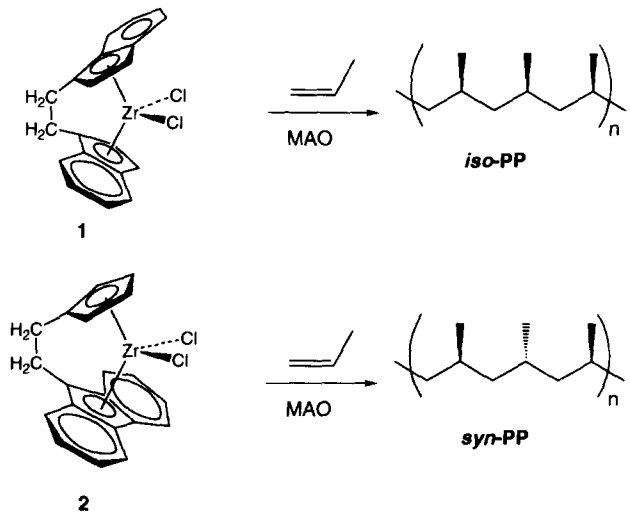

1

2

can be expected that the effect of MAO is to alkylate the metal centre and abstract a chlorine atom, in order to produce the cationic active centre.

The most accepted reaction mechanism for the insertion is the Cossée–Arlman mechanism (Scheme 1) [22–24]. The incoming olefin complexes to the vacant coordination site in **3** forming the π-complex **4**. In the second step the olefin inserts into the metal carbon bond to form the four-membered cyclic transition state **5**. The product **6** resembles the starting structure **3**. A new vacant coordination site is formed to which the next inserting olefin can coordinate to propagate the polymerization further.

Many theoretical investigations have been undertaken to shed light on the insertion mechanism. In this context semiempirical [25–30], ab initio [31–42], density functional theory (DFT) [35,43–46] and molecular mechanics [41,47–57] studies have been published. So far most quantum mechanical investigations have used a methyl group as a model for the polymer chain and generic cyclopentadienyl ligands or chlorine atoms in place of the ligands. Fan et al. studied the insertion of ethylene into Cl_2Ti^+–Et [58]. Comparison of the results clearly indicates that Hartree–Fock investigations overestimate insertion barriers, and that correlated ab initio (MP2) and non-local density functional studies are in good agreement [46] with one another. In the following we discuss briefly the results of a recent DFT investigation on the ethylene insertion into the methyl-zirconocene cation (Fig. 1) [45,59].

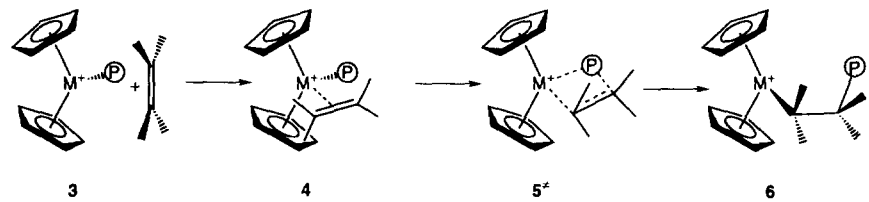

3 4 5≠ 6

Scheme 1. The Cossée–Arlman mechanism [22–24].

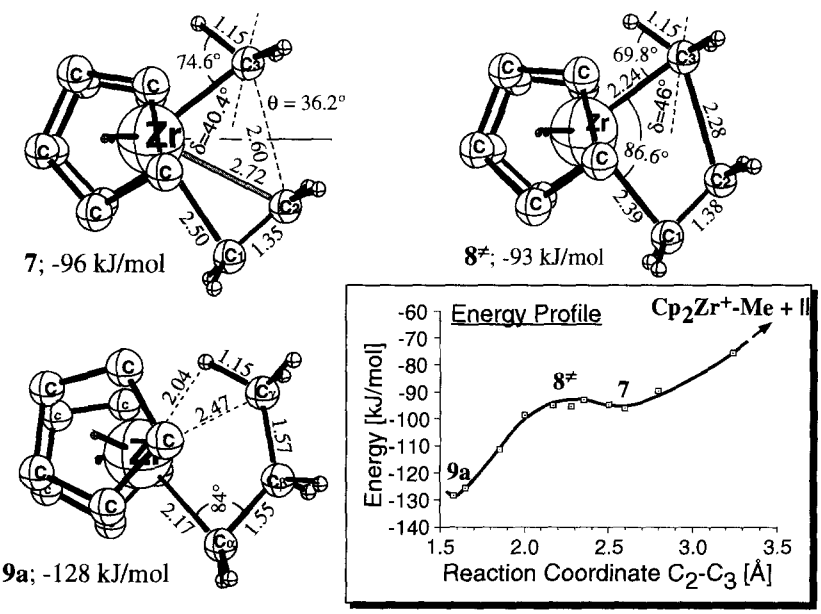

Fig. 1. DFT profile and structures for the ethylene insertion into Cp_2Zr^+–Me; energies in (kJ mol^{-1}), bond lengths in (Å), angles in (deg) [45].

In the first step ethylene binds to the positively charged metal centre in an exothermic reaction forming the π-complex **7**, which is 96 kJ mol^{-1} more stable than the isolated molecules. At this stage of the reaction the methyl group is already tilted ($\delta = 40.4°$) in order to facilitate overlap with the π^*-orbital of the olefin. The transition state **8**$^{\neq}$ for the insertion has an activation barrier of only 3 kJ mol^{-1} relative to the π-complex **7**. The C_2–C_3 distance has shortened to 228 pm and the methyl group is further tilted to the incoming olefin ($\delta = 46°$). This allows the formation of an α-agostic interaction, which seems to facilitate the insertion. The γ-agostic primary product **9a** is 32 kJ mol^{-1} more stable than the π-complex **7** (i.e. −128 kJ mol^{-1} relative to the isolated educts). Thus the insertion is strongly exothermic.

Investigation of other product conformations (Fig. 2) indicates that the primary product **9a** is not the most stable conformation. In the C_s-symmetric structure **9a** rotation around the C_β–C_γ bond minimizes many unfavourable eclipsing interactions that are present, but simultaneously results in a loss of the γ-agostic interaction yielding **9b** (−0.3 kJ mol^{-1}). The most stable conformation **9d** results from a 60° rotation around C_α–C_β. This asymmetric structure shows a strong β-agostic interaction and has no eclipsing interactions. **9d** is 22 kJ mol^{-1} more stable than the primary product **9a** and it has been assumed that **9d** serves as a good model for the resting state between two insertions. Weiss et al. [35] found in addition to the shown structures an α-agostic conformer for Cp_2Ti^+–Pr, which is 17.8 kJ mol^{-1} higher in energy than the corresponding β-agostic structure at the LDF level of theory.

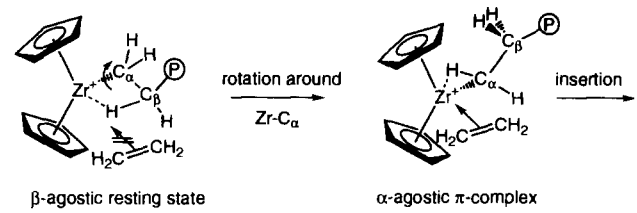

Scheme 2. Rotation around Zr–C_α.

It has been assumed that the experimentally estimated [60] propagation barrier of 31 kJ mol^{-1} does not result from the insertion itself (the calculated barrier [35,43,45] is in the region of 3–5 kJ mol^{-1}) but from a rotation around Zr–C_α. This rotation is necessary in order to move the polymer chain out of the plane and allow bond formation between C_α and the next inserting olefin (Scheme 2).

Since the most stable product conformation [31,45] is a β-agostic structure **9d**, a β-agostic ethyl zirconocene is a better model for the active species into which the olefin inserts. In this paper we present the results of DFT calculations on the reaction of ethylene with the ethyl-zirconocene cation. We comment on the implications of an assumed backside attack for the stereochemistry of the propene polymerization. Finally three possible chain termination processes are compared.

In this investigation we have adopted the model of an unassociated cationic active species. The active role of the cocatalyst, counter ion, or solvent in the catalytic process has been neglected because it would be impractical to include these components in the calculation with the present computational resources available.

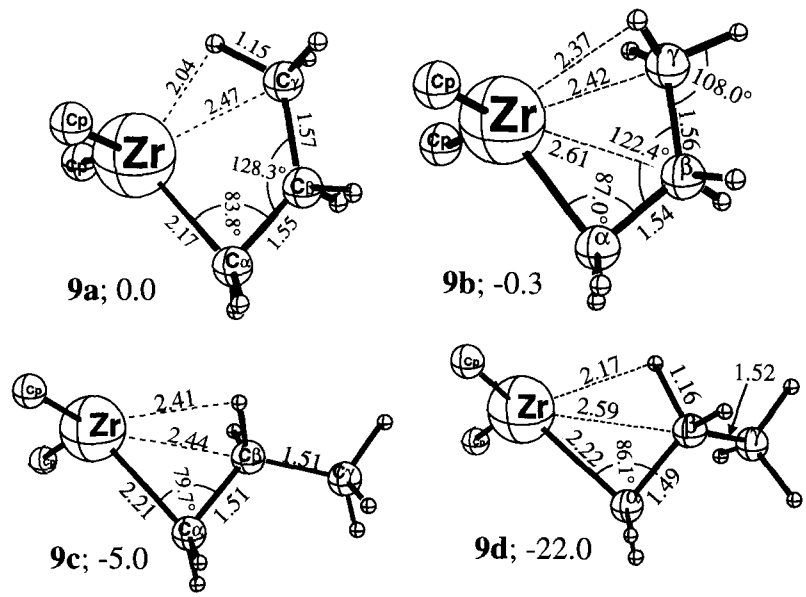

Fig. 2. Conformations of Cp_2Zr^+–Pr **9**; energies in (kJ mol^{-1}), bond lengths in (Å) [45].

2. Computational details

The reported density functional calculations were all carried out using the program systems AMOL [61,62] or ADF 1.1.2 [63], developed by Baerends et al. and vectorized by Ravenek [64]. The numerical integration procedure applied for the calculations was developed by te Velde et al. [65,66]. The geometry optimization procedure was based on the method developed by Verluis and Ziegler [67]. The electronic configurations of the molecular systems were described by an uncontracted triple-ζ STO basis set [68,69] on the zirconium for 4s, 4p, 4d, 5s and 5p. Double-ζ STO basis sets [68,69] were used for carbon (2s, 2p) and hydrogen (1s), augmented with a single 3d or 2p polarization function respectively. Polarization functions were not employed for the carbons and hydrogens on the Cp rings. The $1s^2 2s^2 2p^6 3s^2 3p^6 3d^{10}$ configuration on zirconium, the $1s^2$ configuration on carbon were assigned to the core and treated by the frozen-core approximation [62]. A set of auxiliary [70] s, p, d, f and g STO functions, centred on all nuclei, was used to fit the molecular density and represent Coulomb and exchange potentials accurately in each SCF cycle. Energy differences were calculated by including the local exchange-correlation potential by Vosko et al. [71] with Becke's [72] non-local exchange correction and Perdew's [73] non-local correlation correction. Geometries were optimized without including non-local corrections. Transition states were localized with the following procedure. In the first step all variables but the reaction coordinate were optimized and the reaction coordinate was stepwise decreased. The maximum of this linear transit served as the starting structure in the transition state search without geometry constraints other than mentioned below.

All optimizations were carried out under the assumption of local C_5-symmetry for the Cp-rings. No other constraints were applied.

3. Reaction of Cp_2Zr^+–Et with ethylene

The ethyl complex Cp_2Zr^+–Et may be attacked in two possible approaches (Scheme 3): (A) complexation of the olefin to the frontside of the ethyl-zirconocene or (B) attack at the backside of the β-agostic resting state. There are two possible frontside π-complexes: (i) an α-agostic complex may be formed after rotation around $Zr–C_\alpha$ moving C_β out of the plane. Olefin insertion starting from this α-agostic π-complex is in accordance with the generally assumed insertion pathway and will yield a γ-agostic product. In the following we refer to this reaction as the frontside insertion. (ii) If no rotation occurs, a β-agostic π-complex will emerge and further approach of the olefin will result in hydrogen exchange from the ethyl group to the olefin. This would be a chain termination reaction giving rise to a vinyl-terminated polymer chain and an ethyl zirconocene which can potentially start a new polymer chain.

Backside attack, however, allows insertion without rotation around the $Zr–C_\alpha$ bond. In this case the polymer chain (the ethyl group in our model) has to move to the other side of the plane formed from the metal and the Cp centroids (Cen) in order to allow complexation of the olefin. Insertion will lead to a δ-agostic product.

In the following we discuss the structure of the cationic ethyl zirconocene, the inversion profile, and the calculated reaction profiles for each of the aforementioned pathways.

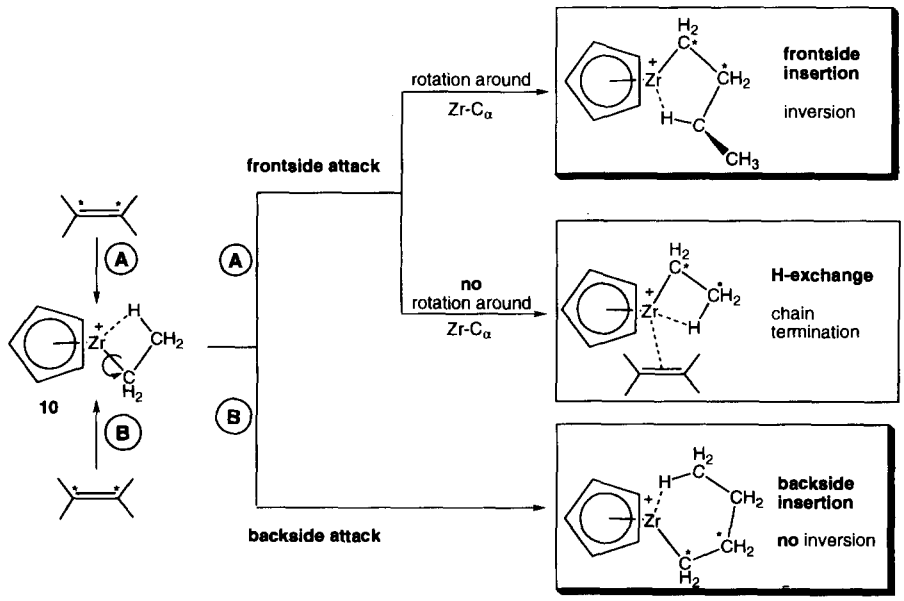

Scheme 3. Possible reactions of Cp_2Zr^+–Et **10** with ethylene.

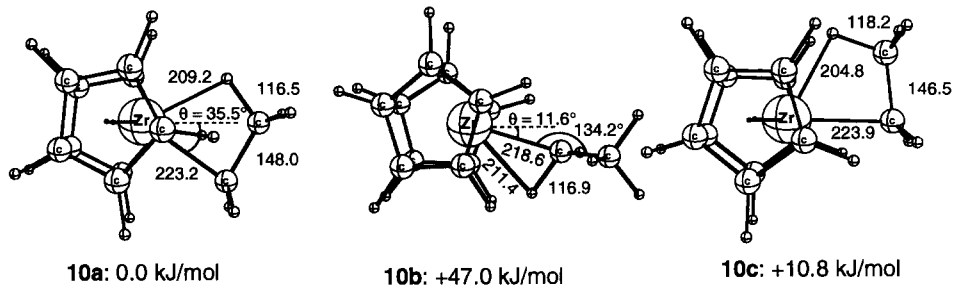

Fig. 3. Structures of Cp_2Zr^+–Et **10a–10c**; relative energy in (kJ mol^{-1}), bond lengths in (pm), angles in (deg).

3.1. The structure of Cp_2Zr^+–Et

The possible structures of the cationic ethyl zirconocene **10** is shown in Fig. 3.

10a is a bent sandwich structure which is in agreement with earlier studies [45]. The ethyl group is bent 35.5° out of the Cen–Zr–Cen plane. The structure is C_s-symmetric and shows a β-agostic interaction, which is obvious from the short zirconium–hydrogen distance (209.2 pm) and an elongated C–H bond (116.5 pm). The β-agostic interaction yields a zirconium centre with near perfect tetrahedral coordination. All other geometrical features agree with structures published before [45] and are therefore not discussed here.

The α-agostic structure **10b** is 47.0 kJ mol^{-1} higher in energy than the β-agostic resting state. Rotation around $Zr–C_\alpha$ puts the β-methyl group closer to the Cp-rings, the resulting unfavourable steric interaction is minimized by an opening of the $Zr–C_\alpha–C_\beta$ angle to 134.2°. At the same time the angle θ decreased to 11.6°. The structure has lost the β-agostic interaction but is stabilized by a strong α-agostic interaction, which is expressed in a long C–H bond (116.9 pm) and a short Zr–H distance (211.4 pm).

For the backside insertion it is necessary that the ethyl group moves around the metal centre in order to make room for the incoming olefin. We investigated this near inversion at the metal centre with the intention of obtaining an estimate of the energy needed for this distortion. Fixing the out-of-plane angle to 0° gave structure **10c** which is only 10.8 kJ mol^{-1} higher in energy than the undistorted **10a**. Thus the movement of the ethyl group is relatively facile. In **10c** the β-agostic interaction is even stronger than in **10a**, which is expressed in a shortened Zr–H distance (204.8 pm) and a longer C–H bond (118.2 pm).

3.2. Frontside insertion of ethylene into Cp_2Zr^+–Et

In this section we present the results of our investigations of the frontside insertion of ethylene. The calcu-

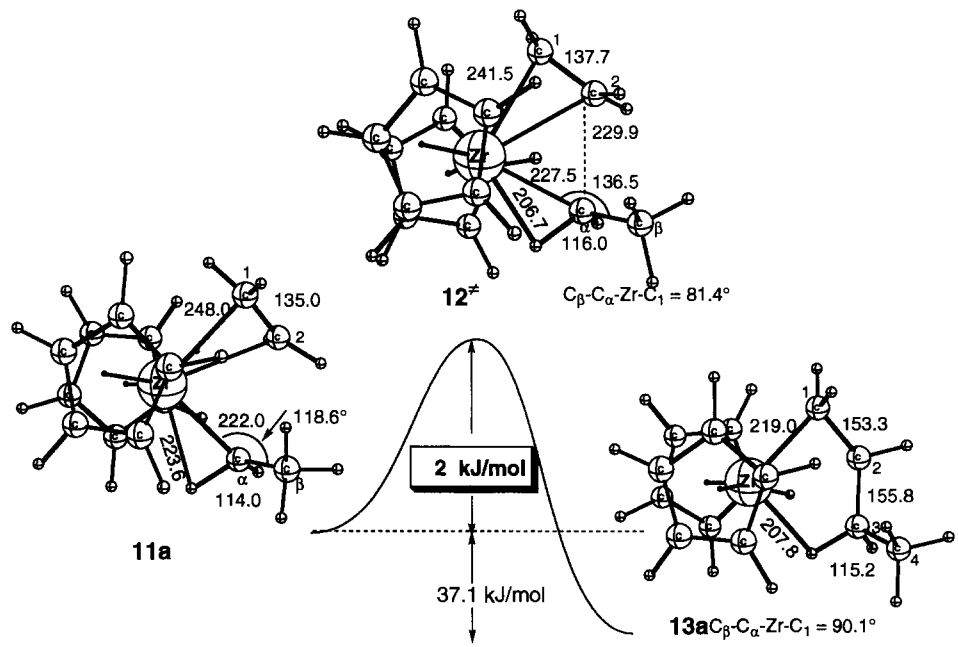

Fig. 4. Stationary points and schematic reaction profile for the frontside insertion; relative energy in (kJ mol^{-1}), bond lengths in (pm), angles in (deg).

lated reaction profile together with the stationary points are shown in Fig. 4.

The π-complex **11a** is formed in an exothermic reaction ($\Delta H = -81.7$ kJ mol^{-1}) from the α-agostic resting state **10b**. The short olefin C–C distance of 135.0 pm in **11a** compared with 132.2 pm in free ethylene shows that there is little back bonding from the metal centre to the π^* olefin orbital. In **11a** the ethyl group has further moved out of the Cen–Zr–Cen plane by 46.5° in order to accommodate the olefin. In the transition state **12**$^{\neq}$ the β-methyl group is rotated out of the plane by 81.4°. Simultaneously the olefin is rotated by 8.4° around the Zr–C_1 bond, moving C_2 below the plane. This rotation acts to minimize steric interactions between the methyl group and the olefin. The large C_α–C_2 distance of 229.9 pm in **12**$^{\neq}$ shows that this is an early transition state. The activation barrier for the insertion amounts to 2 kJ mol^{-1} which is in accordance with earlier calculations [45], see Fig 1. The rotation around Zr–C_α allowed the formation of an α-agostic interaction with a zirconium–hydrogen distance of 206.7 pm and an elongated C_α–H bond (116.0 pm). Unfavourable steric interactions between the cyclopentadienyl rings and the β-methyl group are minimized by formation of a large Zr–C_α–C_β angle (136.5°).

The product of the insertion is the γ-agostic structure **13a**, which is 37.1 kJ mol^{-1} more stable than the π-complex **11a**. Hence the reaction is strongly exothermic. **13a** is asymmetric with the methyl group pointing out of the plane. Unfavourable eclipsing interactions are minimized by formation of a twisted five-membered ring (Zr–C_1–C_2–C_3 = −32.5°, C_1–C_2–C_3–H = 43.6°).

From the results presented in this section it is clear that frontside insertion is a favourable reaction in spite of the rotation around the Zr–C_α bond, which has to occur before the reaction can take place. The steric interactions encountered during this rotation result in the high relative energy of the α-agostic resting state which is 47.0 kJ mol^{-1} less stable than the β-agostic resting state. One has to consider hydrogen exchange to the olefin as an alternative route since a β-agostic frontside π-complex is likely to form from the (more stable) β-agostic resting state. This process is described in the following section.

3.3. The hydrogen exchange reaction

The β-agostic frontside π-complex **11b** can lead to another reaction as mentioned earlier. The short distance between the olefinic C_2 and the β-hydrogen points to a possible reaction of the olefin with the polymer chain end under H-exchange. The calculated reaction profile is shown in Fig. 5.

The π-complex **11b** is formed from the β-agostic resting state **10a** in an exothermic reaction (37.1 kJ mol^{-1}), and the β-agostic interaction is preserved (Zr–H = 205.4 pm, C–H = 117.9 pm). The complex **11b** is virtually C_s-symmetric and the β-hydrogen points to the complexed olefin. The β-agostic π-complex is 3 kJ mol^{-1} more stable than the α-agostic structure **11a**. Starting from **11b** further approach of the olefin without rotation around Zr–C_α directly leads to the transition state **14**$^{\neq}$ with an activation barrier of 29.8 kJ mol^{-1}. The transition state is C_2-symmetric and degenerate. The most remarkable feature of the transition state is the

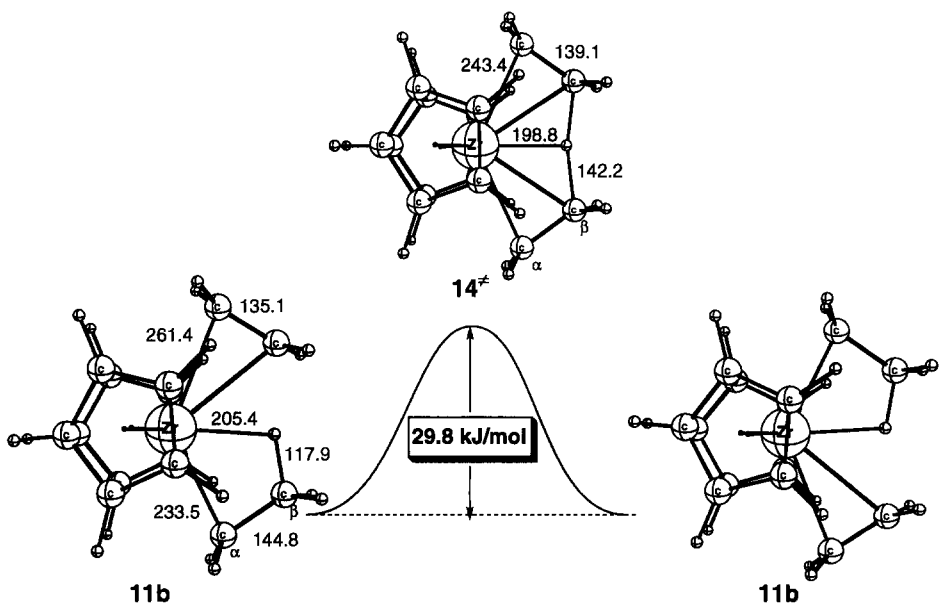

Fig. 5. Stationary points and schematic reaction profile for the H-exchange; relative energy in (kJ mol^{-1}), bond lengths in (pm), angles in (deg).

long C–H bond of 142.2 pm and the short Zr–H distance of only 198.8 pm. This indicates that the β-agostic interaction present in the π-complex **11b** supports the H-transfer from ethyl to ethylene. In the transition state **14**$^{\neq}$ the olefin C–C bond is considerably longer than in free ethylene and the C_α–C_β bond is shortened. Since we were investigating the reaction of an ethyl complex with ethylene, the product of the reaction is identical with the initial π-complex **11b**. One should keep in mind at this point that the ethyl group served as a model for the polymer chain. Thus the complexed ethylene in the product has to be considered as a model for a vinyl-terminated polymer chain. After dissociation an ethyl-zirconocene would be formed which can potentially serve as initiator for a new polymer chain. The low activation barrier of 29.8 kJ mol^{-1} clearly proves that this is a feasible chain termination reaction. Hydrogen transfer, i.e. chain termination, will take place once the β-agostic frontside π-complex **11b** is formed. We compare three possible chain termination reactions in Section 4.

3.4. The backside insertion of ethylene into Cp_2Zr^+–Et

In this section the results for the backside insertion are presented. The obtained reaction path is depicted in Fig. 6.

Backside attack of ethylene leads to the formation of the π-complex **15** in an exothermic reaction (ΔH = −42.3 kJ mol^{-1}). The backside complex **15** is even more stable than the β-agostic frontside complex **11b** by 5.2 kJ mol^{-1} and at −8.2 kJ mol^{-1} relative to the front side α-agostic π-complex **11a**. This again strengthens the earlier assumption that the wagging motion of the ethyl group is facile and does not require much energy. In **15** the ethyl group has moved even further to the other side (θ = −24.6°) in order to accommodate the olefin. In the β-agostic frontside π-complex **11b** the ethyl group has moved in the other direction pushing the α-hydrogens closer to the Cp-rings, whereas in the backside complex **11b** only one β-hydrogen atom points between the rings. We assume that the reason for the slightly higher relative energy of the frontside π-complex is the steric interaction of the α-hydrogens with the ligands. In the backside π-complex **15** the β-agostic interaction is retained as indicated by a long C–H bond (116.4 pm) and a short Zr–H distance (204.5 pm). The olefin binds weakly to the metal (Zr–C_1 = 256.2 pm, Zr–C_2 = 265.9 pm, C_1–C_2 = 135.4 pm) and the complex is practically C_s-symmetric.

Only 28.9 kJ mol^{-1} are needed to reach the transition state **16**$^{\neq}$ for the backside insertion. The relatively short C_2–C_α distance of 202.2 pm and the elongated C_1–C_2 bond (140.8 pm) point to an advanced transition state. **16**$^{\neq}$ is asymmetric with respect to the zirconium-alkyl ring fused by the β-hydrogen, which allows an almost perfectly staggered structure. We would like to point out that once the ethyl group has moved to the other side, the insertion resembles that calculated earlier for the insertion into the methyl complex. The product of the insertion is the δ-agostic structure **13b**, where the ring twist is slightly stronger than in the transition state **16**$^{\neq}$. The δ-agostic interaction is weak, as can be

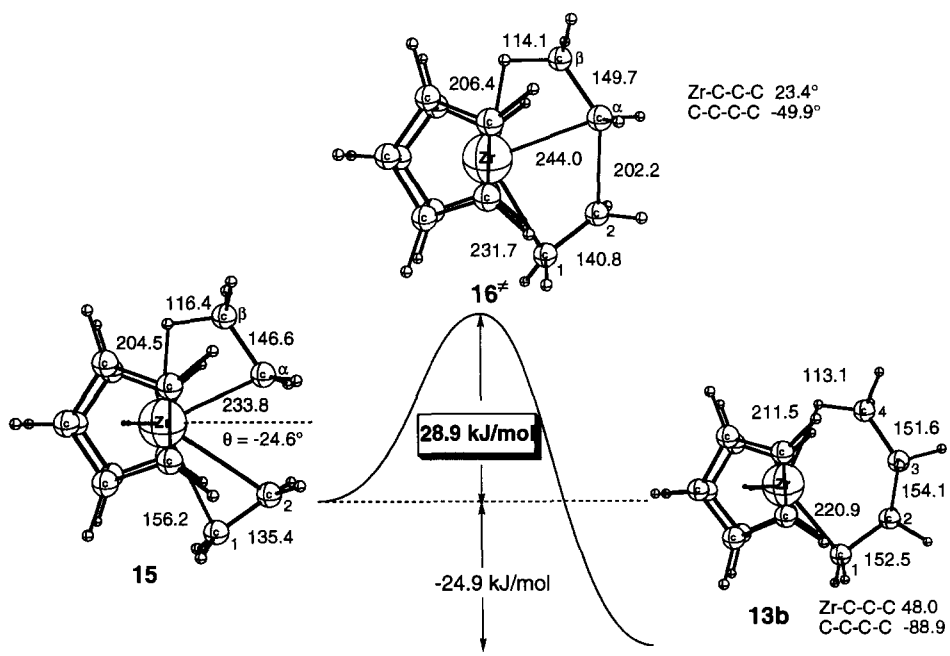

Fig. 6. Stationary points and schematic reaction profile for the backside insertion; relative energy in (kJ mol^{-1}), bond lengths in (pm), angles in (deg).

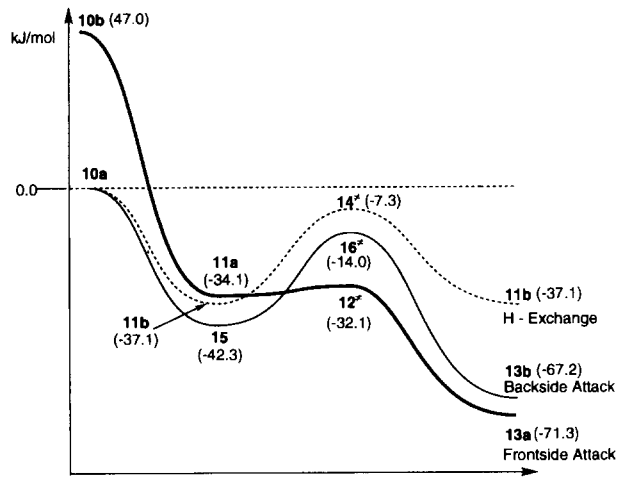

Fig. 7. Calculated reaction profiles for the H-exchange reaction, frontside insertion and the backside insertion. Energies are relative to the β-agostic resting state **10a** and are given in parentheses in (kJ mol^{-1}).

concluded from the short C–H bond (113.1 pm), which might be a reason for the higher energy of **13b** (+4.1 kJ mol^{-1}) relative to the γ-agostic product **13a** of the frontside attack. The product **13b** is 24.9 kJ mol^{-1} more stable than the initial backside π-complex **15**. Thus the overall insertion process is strongly exothermic.

3.5. A comparison of the frontside and backside approaches

A comparison of the three calculated profiles (Fig. 7) makes it evident that insertion into a β-agostic resting state can only occur from the backside, whereas the frontside insertion requires rearrangement of the β-agostic resting state to an α-agostic structure like **10b** prior to or in concert with complexation of the olefin. This rotation is endothermic by 47.0 kJ mol^{-1}. The frontside insertion pathway shows the lowest activation barrier of all processes studied here and is exothermic with respect to the π-complex, but the α-agostic structure **10b** is less stable than the β-agostic conformer **10a**. Thus backside insertion cannot be completely excluded in spite of the higher activation energy compared with the frontside insertion.

The presented calculations show that starting from the β-agostic frontside π-complex, hydrogen exchange has a small activation barrier and thus chain termination is a possible outcome. The significance of this chain terminating reaction in comparison with other mechanisms is discussed later.

We now comment on the consequences of an assumed backside insertion for the stereoselective propene polymerization. So far the stereochemistry of the insertion has only been interpreted in terms of the frontside attack. The results are summarized briefly in Scheme 4.

From Scheme 4 as well as Fig. 1 it is evident that frontside insertion is accompanied with an inversion at the metal centre, i.e. the polymer chain moves back and forth with every olefin insertion. This causes the olefin to attack from alternating sides. In the case of backside insertion (Fig. 6), however, the polymer chain stays on one side of the catalyst for the length of the polymerization, i.e. every olefin attacks from the same side. This is important for interpretation of the stereo-determining factors, especially for the *syndio*selective propene polymerization.

First we describe the isospecific propene polymerization in terms of the frontside attack. So far most isospecific catalysts exhibit a local C_2-symmetry, as there are for example the *ansa*-bis(indenyl)-ligands introduced by Kaminsky and Brintzinger [2]. The most accepted stereo-control mechanism is site-control [5,52,53,74], i.e. it is assumed that the ligands influence directly the facial preference of the incoming olefin (*re-* or *si-*). This is demonstrated in (1). Propene inserts such that the methyl-group points away from the larger ligand (in this case the lower side); at the same time inversion at the metal takes place, putting the polymer chain to the

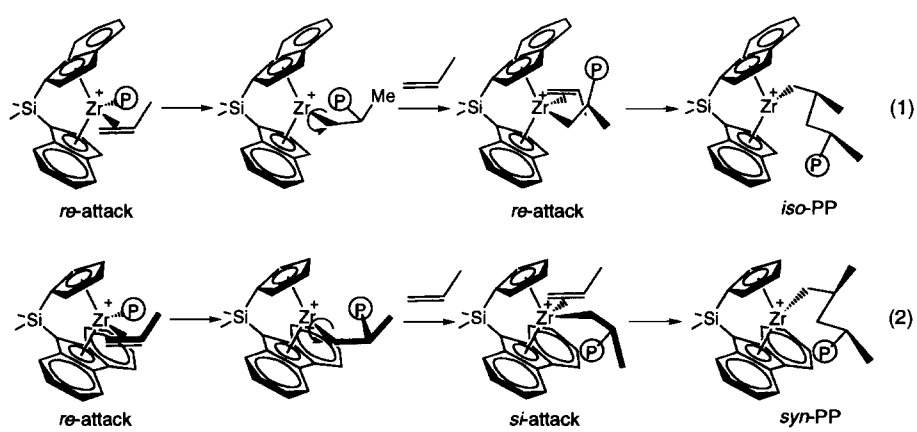

Scheme 4. Site-control in *iso-* and *syndio*-selective catalysts under the assumption of frontside insertion.

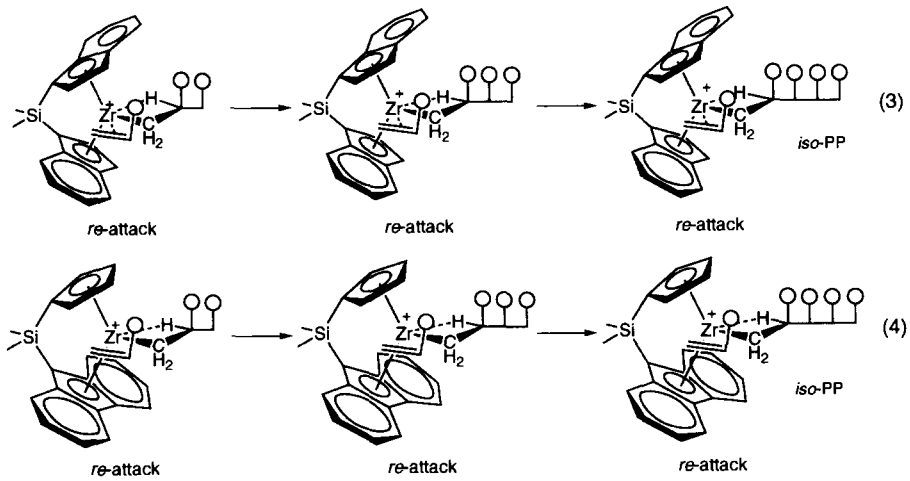

Scheme 5. Site-control in *iso*- and *syndio*-selective catalysts under the assumption of backside insertion.

front. In the next step the olefin attacks from behind, with the methyl group pointing down this time. This makes it clear why C_2-symmetric catalysts yield *isotactic* polypropene. The same explanation holds for the *syndiotactic* propene polymerization utilizing Ewen's [3] C_s-symmetric catalyst (2). As before the olefin will insert with the methyl group pointing away from the larger ligand side (with its *re*-side in our drawing, the methyl group up). Inversion at the metal centre now puts the polymer chain in another enantiomorphic surrounding. The next propene will be complexed with its *si*-side (methyl up) and insertion leads to *syndiotactic* polypropene. There have been other publications arguing with chain-end-control [5,50,75], i.e. the chiral polymer chain controls the directionality of the olefin.

Do the same arguments hold for the backside attack? In Scheme 5 we have sketched the expected results based on site-control.

From reaction (3) it becomes clear that the isotactic polymerization can be explained with site-control. The olefin will attack from the same side at every step, putting the propene-methyl group in an identical environment. Thus the olefin will insert with the same facial preference (*re*) at every point of the polymerization yielding *isotactic* polypropene. However, the same preference should be expected for the *syndioselective* catalyst, since without inversion at the metal the olefin will enter from the same enantiomorphic side, leading to *isotactic* polypropene. Thus at least for the *syndioselective* polymerization other interactions have to be

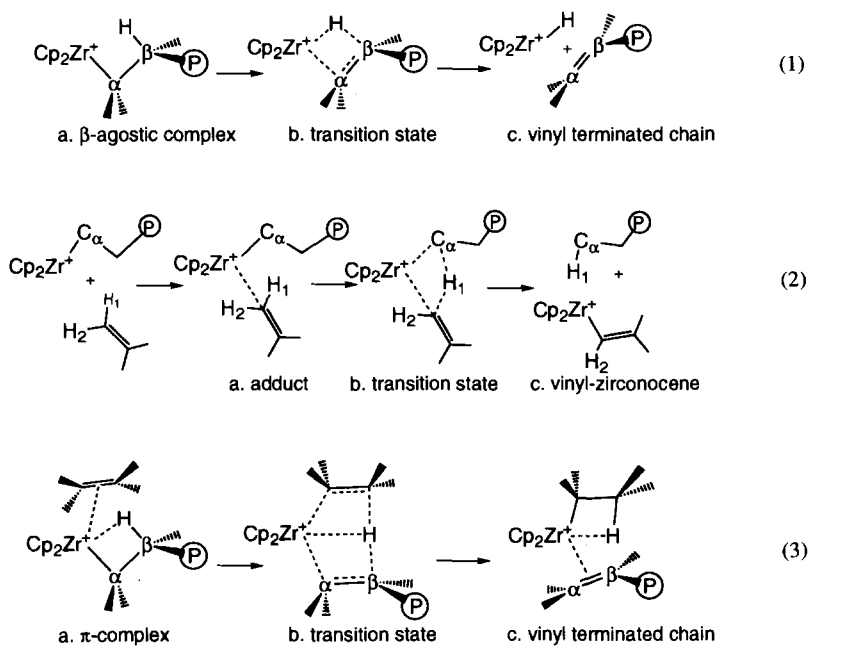

Scheme 6. Chain termination reactions.

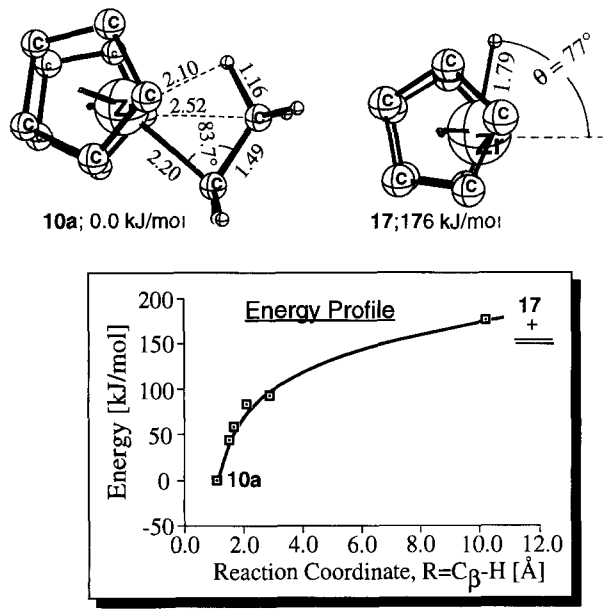

Fig. 8. DFT profile and stationary points for the β-hydride elimination [45], bond lengths in (Å), angles in (deg).

considered in the case of backside attack! As mentioned before, some authors discussed chain-end-control as another possible mechanism.

4. Chain termination reactions

In this section we compare computational data for three important chain termination reactions. Many investigations assumed β-hydride elimination as the major chain-terminating mechanism [76]. Other discussed processes include olefin C–H-activation and the hydrogen-exchange [9,77,78] as studied in this paper. The first two processes have been studied with DFT methods before [45] and the results are compared with those obtained for the H-exchange. The three reactions are shown schematically in Scheme 6.

The β-hydride elimination (1) can be considered as an extreme form of a β-agostic interaction, where the hydrogen is completely transferred to the metal. In the transition state the metal–carbon and the carbon–hydrogen bonds should be broken yielding a metal hydride and a vinyl-terminated polymer chain. The metal-hydride then can start a new polymer chain.

In the alkene C–H bond activation (2) the olefin approaches the metal centre with the protons pointing to the metal rather than with the π-bond. An adduct is formed and in the transition state one hydrogen atom is transferred from the olefin to the polymer chain in a σ-bond metathesis reaction. The products are a saturated polymer chain and a vinyl metallocene. The vinyl metallocene may further polymerize olefin yielding a vinyl end group.

The hydrogen-exchange reaction (3) has been discussed in detail in Section 3. The olefin approaches the metal centre from its frontside and forms a π-complex. In the transition state the β-hydrogen is transferred to the olefin and a vinyl-terminated polymer chain is eliminated. The newly formed alkyl-metallocene than can start a new chain.

Woo et al. [45] investigated the first two pathways by means of DFT. The calculated profile for the β-hydride elimination is shown in Fig. 8.

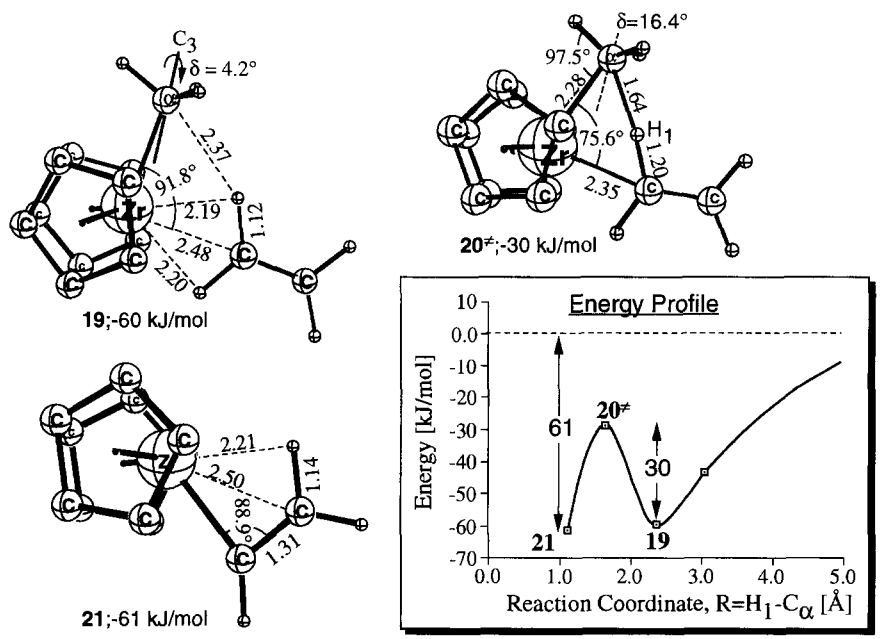

Fig. 9. The DTF profile for the C–H activation reaction [45], bond lengths in (Å), angles in (deg).

The profile shows no transition state and the energy rises steadily when the C_β–H distance in the β-agostic ethyl complex **10a** is elongated until the zirconocene-hydride **17** is isolated from the eliminated ethylene. The final products are 176 kJ mol^{-1} higher in energy than the initial alkyl-zirconocene. This clearly rules out the β-hydride elimination as a feasible pathway for chain termination.

The olefin C–H activation has been studied by Woo et al. [45] for the methyl-zirconocene **18**. The DFT profile and stationary points are summarized in Fig. 9.

The initial adduct **19** is 60 kJ mol^{-1} more stable than the isolated molecules. It is thus of higher energy than the π-complex **7** for which the corresponding stability is 96 kJ mol^{-1}. The ethylene is complexed through agostic interactions to the metal centre. As a second source of stability the authors state electrostatic interactions with the electron-deficient metal. The activation barrier for the four-centred transition state **20**$^{\neq}$ amounts to 30 kJ mol^{-1}. In the transition state the C_1–Zr distance has shortened (235 pm) while the H_1 approaches the methyl group (C_α–H_1 = 164 pm, C_1–H_1 = 120 pm). As in the insertion reaction, the methyl group is tilted ($\delta = 16.4°$) to allow overlap with the proton and to form a weak α-agostic interaction. The vinyl product **21** finally is 1 kJ mol^{-1} more stable than the initial adduct **19**. The activation barrier is moderate and the reaction is exothermic with respect to the isolated molecules. Thus, from both a kinetic and thermodynamic viewpoint, this model indicates that chain termination by C–H activation is much more favourable than by β-hydride elimination. However, one has to consider that for the reaction with longer chains, rotation around Zr–C_α has to take place in order to allow overlap of the olefin with the α-carbon. This may be overcome in a backside C–H activation.

None of these problems arises in the H-exchange reaction. As outlined in Section 3, H-exchange easily takes place from a frontside π-complex. No costly rotations are involved and the reaction is exothermic with respect to the educts. Furthermore the activation barrier (29.8 kJ mol^{-1}) for the H-exchange is lower than for the C–H-activation process (31.0 kJ mol^{-1}). In the H-exchange reaction a hydrogen is transferred from the polymer chain end to the olefin, leading to vinyl terminated chains and an alkyl-zirconocene, which starts a new polymer chain. Experimental end group determinations are consistent with this: Giardello et al. [79] found that polypropene-chains contain a vinyl and a propene end group.

One can explain the experimentally observed dependence of the molecular weight on the substitution of the ligands with this mechanism. It has been observed that methyl-substitution at each 2-position of the C_5 ring in *ansa*-zirconocenes increases the molecular weight [4,6,8,80]. The molecular weight of polymers depends on the rate of insertion relative to chain termination. Since the H-exchange reaction starts with the formation of a frontside complex, the olefin will experience the steric bulk of ligands at the 2-position. Increased steric demand, as through introduction of a methyl group, will make the complexation and the further reaction form the frontside more difficult (Scheme 7). This will slow down the chain termination reaction relative to the insertion and thus lead to higher molecular weights. Both the frontside and backside insertions are affected less significantly by this substitution.

5. Concluding remarks

We have investigated the reaction of Cp_2Zr^+–Et with ethylene. This is the first computational study on metallocenes utilizing an ethyl group as a model for the polymer chain. This was necessary, since from earlier work it can be assumed that the resting state between two insertions is a β-agostic structure. The corresponding α-agostic structure is calculated to be 47.0 kJ mol^{-1} less stable, which is in agreement with earlier work [35]. In accordance with other theoretical investi-

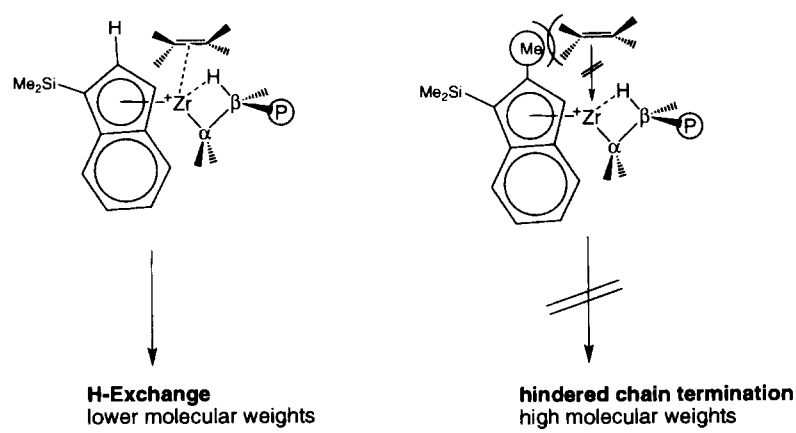

H-Exchange
lower molecular weights

hindered chain termination
high molecular weights

Scheme 7. The effect of methyl-substitution on the molecular weight.

gations, the frontside insertion has a low activation barrier of 2 kJ mol^{-1} and is exothermic ($\Delta H = -37.1$ kJ mol^{-1}) relative to the α-agostic π-complex. In order to allow reaction of the olefin with the α-carbon, rotation around $Zr-C_\alpha$ has to take place, putting the β-carbon (of the polymer chain) out of the plane. This introduces a repulsive steric interaction between the β-methyl group and the Cp rings, resulting in a large $Zr-C_\alpha-C_\beta$ angle (136.5°).

Starting from a β-agostic π-complex, chain termination via hydrogen exchange can take place. Without rotation around $Zr-C_\alpha$ the β-agostic hydrogen is transferred from the chain end to the approaching olefin with an activation barrier of 29.8 kJ mol^{-1}. The studied reaction is thermoneutral with respect to the π-complex. The H-exchange yields a vinyl-terminated polymer chain and an alkyl-zirconocene, which can act to polymerize further olefin. We conclude that starting from a frontside β-agostic π-complex, H-exchange chain termination will take place, whereas for insertion and chain growth it is necessary to form an α-agostic π-complex.

Backside attack of an olefin leads to the formation of a π-complex in which the ethyl group has moved around the zirconium in order to make room for the olefin. The activation energy for the insertion is 28.9 kJ mol^{-1} and the overall reaction is exothermic by 24.9 kJ mol^{-1}. This is in good agreement with the experimental estimate of the propagation barrier of ca. 30 kJ mol^{-1} [60]. Insertion barriers calculated for ethylene insertions into methyl-zirconocenes have been in the range of 0–4 kJ mol^{-1} and a rearrangement of the product has been assumed to be responsible for the higher experimentally determined barrier [35,45], which is in agreement with the results for the frontside insertion presented in this paper. The product of the backside insertion is a δ-agostic structure.

In contrast to the frontside insertion, backside attack does not involve inversion at the metal centre. Thus the olefin will approach the catalytic centre from the same side at every insertion step. The formation of isotactic polypropene is in agreement with the so far accepted site-control mechanism, because the inserting propene experiences identical interactions at each step. However for the formation of syndiotactic polypropene it is necessary that the chemical environment alternates. This can only be achieved by the assumption of a chain-end control in the case of backside attack.

We carried out force-field calculations on the propene insertion into the *syndio*-selective $SiMe_2(Cp)(Flu)Zr^+$-catalyst[3] in order to test this assumption [81]. The model system included a *syn*-polypropene chain of three propene units. The calculations revealed (1) that β- and γ-agostic orientations of the polymer chain are predominant and (2) that from one insertion to the other the chain moves up and down relative to the ligand system. From this we conclude that for the propene insertion two orientations alternate. In the first step the polymer chain points to the larger ligand side and the propene methyl group points away from the fluorenyl-ligand and the polymer chain. The next insertion is governed by a stronger interaction of the propene with the polymer chain than with the ligand, i.e. the methyl group points away from the polymer to the fluorenyl rings.

Although these molecular mechanics calculations of the possible π-complexes do not clearly differentiate between *iso*- and *syndio*-tactic insertion for the second step, it can be assumed that the discrimination might become stronger when the transition state is investigated. We intend to explore this possibility also by means of molecular mechanics calculations.

If syndiospecific α-olefin polymerization can be shown to occur through the backside attack via chain end control, then the backside insertion is clearly a feasible chain propagation mechanism. The important question that arises is which insertion process dominates, the frontside attack or the backside attack? The frontside attack has an extremely small insertion barrier of 2 kJ mol^{-1} whereas the backside attack has a significantly larger 28.9 kJ mol^{-1} insertion barrier. However, the frontside insertion requires formation of the α-agostic π-complex and therefore demands an unfavourable rotation of the polymer chain about the $M-C_\alpha$ bond. The α-agostic π-complex **11a** can form in several ways: (1) from the π-complex **11b** by rotation about the $M-C_\alpha$ bond, or (2) by first formation of the α-agostic resting state **10b**, followed by olefin complexation, or (3) by some concerted process whereby the incoming olefin induces $M-C_\alpha$ rotation. In any case, the required rotation about the $M-C_\alpha$ bond is unfavourable since steric interactions between the polymer chain and the Cp ligands of the metallocene occur. Therefore, the overall propagation barrier in the frontside attack is not due to the insertion process, but rather some rearrangement process involving rotation about the $M-C_\alpha$ bond. Unfortunately, we have not explored such rearrangement processes in this study. However, we have previously compared the $M-C_\alpha$ bond rotation for several bis-Cp metallocenes and mono-Cp constrained geometry catalysts using molecular mechanics [43,44]. In order to compare more conclusively the frontside and backside mechanisms, we will have to obtain a more complete picture of the frontside propagation energy profile including the rearrangement processes which give rise to the α-agostic π-complex. We are currently investigating such rearrangement processes with both molecular mechanics and density functional theory.

Three possible chain termination reactions have been compared: β-hydride elimination, C–H-activation and H-exchange. Earlier calculations made it clear that the β-hydride elimination is very unfavourable because it is

strongly endothermic ($\Delta H = +176$ kJ mol^{-1}). Olefin C–H-activation has a relatively low activation barrier of 31 kJ mol^{-1} and is exothermic with respect to the isolated reaction partners. However, for the reaction to take place from the frontside, rotation around Zr–C_α has to occur. Furthermore, the adduct **19** is less stable than the β-agostic frontside π-complex **11b**. The H-exchange reaction studied in this paper has an activation barrier of 29.8 kJ mol^{-1}, the reaction path does not involve any rotations and starts from the more stable β-agostic frontside π-complex **11b**. We therefore consider the H-exchange reaction as the most probable chain-terminating process.

Acknowledgments

This investigation was supported by the Natural Science and Engineering Research Council (NSERC) of Canada as well as the Donars of the Petroleum Research Fund, administered by the American Chemical Society (ACS-PRF #27023-AC3). J.C.W. Lohrenz wishes to thank the Fond der Chemischen Industrie who supported this work with a generous Liebig-Stipendium.

References

[1] A. Andersen, H.-G. Cordes, J. Herwig, W. Kaminsky, A. Merck, R. Mottweiler, J. Pein, H. Sinn and H.-J. Vollmer, *Angew. Chem., 88* (1976) 689.
[2] W. Kaminsky, K. Külper, H.H. Brintzinger and F.R.W.P. Wild, *Angew. Chem., 97* (1985) 507.
[3] J.A. Ewen, R.L. Jones, A. Razavi and J.D. Ferrara, *J. Am. Chem. Soc., 110* (1988) 6255.
[4] T. Mise, S. Miya and H. Yamazaki, *Chem. Lett.* (1989) 1853.
[5] J.A. Ewen, *J. Am. Chem. Soc., 106* (1984) 6355.
[6] W. Röll, H.-H. Brintzinger, B. Rieger and R. Zolk, *Angew. Chem., 102* (1990) 339.
[7] W. Spaleck, M. Antberg, M. Aulbach, B. Bachmann, V. Dolle, S. Haftka, K. Küber, J. Rohrmann and A. Winter, in *40 Years Ziegler Catalysts*, Freiburg, 1993, in press.
[8] W. Spaleck, F. Küber, A. Winter, J. Rohrmann, B. Bachmann, M. Antberg, V. Dolle and E.F. Paulus, *Organometallics, 13* (1994) 954.
[9] U. Stehling, J. Diebold, R. Kirsten, W. Röll, H.-H. Brintzinger, S. Jüngling, R. Mülhaupt and F. Langhauser, *Organometallics, 13* (1994) 964.
[10] B.J. Burger, M.E. Thompson, W.D. Cotter and J.E. Bercaw, *J. Am. Chem. Soc., 112* (1990) 1566.
[11] P.J. Shapiro, W.D. Cotter, W.P. Schaefer, J.A. Labinger and J.E. Bercaw, *J. Am. Chem. Soc., 116* (1994) 4623.
[12] P.L. Watson, *J. Am. Chem. Soc., 104* (1982) 337.
[13] G. Jeske, H. Lauke, H. Mauermann, P.N. Swepston, H. Schumann and T.J. Marks, *J. Am. Chem. Soc., 107* (1985) 8091.
[14] B.J. Thomas and K.H. Theopold, *J. Am. Chem. Soc., 110* (1988) 5902.
[15] K.H. Theopold, R.A. Heintz, S.K. Noh, and B.J. Thomas (eds.), *Homogeneous Chromium Catalysts for Olefin Polymerization*, Vol. 230 ACS, Washington, DC, 1992.
[16] G.F. Schmidt and M. Brookhart, *J. Am. Chem. Soc., 107* (1985) 1443.
[17] M. Brookhart, J.A.F. Volpe, D.M. Lincoln, I.T. Horváth, J.M. Millar, *J. Am. Chem. Soc., 112* (1990) 5634.
[18] R.F. Jordan, *J. Chem. Edu., 65* (1988) 285.
[19] Y.W. Alelynuas, R.F. Jordan, S.F. Echols, S.L. Borkowsky and P.K. Bradley, *Organometallics, 10* (1991) 1406.
[20] P.G. Gassman and M.R. Callstrom, *J. Am. Chem. Soc., 109* (1987) 7875.
[21] R.F. Jordan, C.S. Bajgur, R. Willett and B. Scott, *J. Am. Chem. Soc., 108* (1986) 7410.
[22] P. Cossée, *J. Catal., 3* (1964) 80.
[23] E.J. Arlman, *J. Catal., 3* (1964) 89.
[24] E.J. Arlman and P. Cossée, *J. Catal., 3* (1964) 99.
[25] D.R. Armstrong, P.G. Perkins and J.J.P. Stewart, *J. Chem. Soc., Dalton Trans.*, (1972) 1972.
[26] P. Cassoux, F. Crasnier and J.-F. Labarre, *J. Organomet. Chem., 165* (1979) 303.
[27] R.J. McKinney, *J. Chem. Soc., Chem. Commun.*, (1980) 490.
[28] A.C. Balazs and K.H. Johnson, *J. Chem. Phys., 77* (1982) 3148.
[29] A. Shiga, H. Kawamura, T. Ebara, T. Sasaki and Y. Kikuzono, *J. Organomet. Chem., 366* (1989) 95.
[30] M.-H. Prosenc, C. Janiak and H.-H. Brintzinger, *Organometallics, 11* (1992) 4036.
[31] H. Kawamura-Kuribayashi, N. Koga and K. Morokuma, *J. Am. Chem. Soc., 114* (1992) 8687.
[32] H. Kawamura-Kuribayashi, N. Koga and K. Morokuma, *J. Am. Chem. Soc., 114* (1992) 2359.
[33] H. Fujimoto, T. Yamasaki, H. Mizutani and N. Koga, *J. Am. Chem. Soc., 107* (1985) 6157.
[34] O. Novaro, E. Blaisten-Barojas, E. Clementi, G. Giunchi and M.E. Ruiz-Vizcaya, *J. Chem. Phys., 68* (1978) 2337.
[35] H. Weiss, M. Ehrig and R. Ahlrichs, *J. Am. Chem. Soc., 116* (1994) 4919.
[36] P.E.M. Siegbahn, *Chem. Phys. Lett., 205* (1993) 290.
[37] S. Sakai, *J. Phys. Chem., 95* (1991) 7089.
[38] O. Novaro, *Int. J. Quantum Chem., 42* (1992) 1047.
[39] R.J. Meier, G.H.J.v. Dormaele, S. Iarlori and F. Buda, *J. Am. Chem. Soc., 116* (1994) 7274.
[40] E.P. Bierwagen, J.E. Bercaw and I.W.A. Goddard, *J. Am. Chem. Soc., 116* (1994) 1481.
[41] L.A. Castonguay, and A.K. Rappé, *J. Am. Chem. Soc., 114* (1992) 5832.
[42] C.A. Jolly and D.S. Marynick, *J. Am. Chem. Soc., 111* (1989) 7968.
[43] L. Fan, D. Harrison, T.K. Woo and T. Ziegler, submitted to *Organometallics*.
[44] T.K. Woo, L. Fan and T. Ziegler, in *40 Years Ziegler Catalysts.*, Freiburg, 1993, in press.
[45] T.K. Woo, L. Fan and T. Ziegler, *Organometallics, 13* (1994) 2252.
[46] F.U. Axe and J.M. Coffin, *J. Phys. Chem., 98* (1994) 2567.
[47] L. Cavallo, G. Guerra, P. Corradini, L. Resconi and R.M. Waymouth, *Macromolecules, 26* (1993) 260.
[48] P. Corradini and G. Guerra, *Prog. Polym. Sci., 16* (1991) 239.
[49] G. Guerra, L. Cavallo, G. Moscardi, M. Vacatello and P. Corradini, *J. Am. Chem. Soc., 116* (1994) 2988.
[50] V. Venditto, G. Guerra, P. Corradini and R. Fusco, *Polymer, 31* (1990) 530.
[51] A. Zambelli and P. Ammendola, *Prog. Polym. Sci., 16* (1991) 203.
[52] P. Corradini, G. Guerra, M. Vacatello and V. Villani, *Gazz. Chim. Ital., 118* (1988) 173.
[53] L. Cavallo, G. Guerra, L. Oliva, M. Vacatello and P. Corradini, *Polym. Commun., 30* (1989) 16.

[54] L. Cavallo, P. Corradini, G. Guerra and M. Vacatello, *Polymer*, *32* (1991) 1329.
[55] L. Cavallo, G. Guerra, M. Vacatello and P. Corradini, *Chirality*, *3* (1991) 299.
[56] L. Cavallo, G. Guerra, M. Vacatello and P. Corradini, *Macromolecules*, *24* (1991) 1784.
[57] J.R. Hart and A.K. Rappé, *J. Am. Chem. Soc.*, *115* (1993) 6159.
[58] L. Fan, D. Harrison, L. Deng, T.K. Woo, D. Swerhone and T. Ziegler, *Can. J. Chem.* in press.
[59] T.K. Woo, L. Fan and T. Ziegler, *Organometallics*, *13* (1994) 423.
[60] J.C.W. Chien and A. Razavi, *J. Polym. Sci. A*, *26* (1988) 2369.
[61] E.J. Baerends, D.E. Ellis and P. Ros, *Chem. Phys.*, *2* (1973) 41.
[62] E.J. Baerends, *PhD Thesis*, Vrije Universiteit, 1975.
[63] E.J. Baerends, Vrije Universiteit, Amsterdam, 1994.
[64] W. Ravenek, in H. J.J. t. Riele, T.J. Dekker and H.A. v.d. Vorst (eds.) *Algorithms and Applications on Vector and Parallel Computers*, Elsevier, Amsterdam, 1987.
[65] P.M. Boerrigter, G.t. Velde and E.J. Baerends, *Int. J. Quantum Chem.*, *33* (1988) 87.
[66] G.t. Velde and E.J. Baerends, *J. Comput. Phys.*, *99* (1992) 84.
[67] L. Versluis and T. Ziegler, *J. Chem. Phys.*, *88* (1988) 322.
[68] J.G. Snijders, P. Vernooijs and E.J. Baerends, *At. Nucl. Data Tables*, *26* (1981) 483.
[69] P. Vernooijs, G.J. Snijders and E.J. Baerends, Slater Type Basis Functions for the whole Periodic System, Free University of Amsterdam, Amsterdam, 1981.
[70] J. Krijn and E.J. Baerends, Fit Functions in the HFS-method, Free University of Amsterdam, Amsterdam, 1984.
[71] S.H. Vosko, L. Wilk and M. Nusair, *Can. J. Phys.*, *58* (1980) 1200.
[72] A.D. Becke, *Phys. Rev. A*, *38* (1988) 3098.
[73] J.P. Perdew, *Phys. Rev. B*, *33* (1986) 8822.
[74] P. Longo, A. Grassi, C. Pellecchia and A. Zambelli, *Macromolecules*, *20* (1987) 1015.
[75] A. Zambelli, P. Ammendola, A. Grassi, P. Longo and A. Proto, *Macromolecules*, *19* (1986) 2703.
[76] J.C.W. Chien and B.-P. Wang, *J. Polym. Sci.*, *28* (1990) 15.
[77] J. Boor, *Ziegler–Natta Catalysts and Polymerization*, Academic Press, New York, 1979, p. 258.
[78] T. Tsutui, A. Mizuno and N. Kashiwa, *Polymer*, *30* (1989) 428.
[79] M.A. Giardello, M.S. Eisen, C.L. Stern and T.J. Marks, *J. Am. Chem. Soc.*, *115* (1993) 3326.
[80] W.A. Herrmann, J. Rohrmann, E. Herdtweck, W. Spaleck and A. Winter, *Angew. Chem.*, *101* (1989) 1536.
[81] J.C.W. Lohrenz and T. Ziegler, *ACS Meet., Physical Chemistry, Anaheim, 2–6 April 1995.*